DYNAMIC MODELLING OF A MEGAWATT PEM FUEL CELL SYSTEM WITH HYDROGEN SUPPLY FROM AN LH2 TANK SYSTEM

Bing Ni, Jörg Weiss, Sofiya Pracht, Simon Riedel, Asif Ansar, Cornelie Bänsch

Deutsches Zentrum für Luft- und Raumfahrt e.V. (DLR), German Aerospace Center, Institute of Engineering Thermodynamics, Energy System Integration, Pfaffenwaldring 38-40, 70569 Stuttgart, Germany

Abstract

Nowadays energy supply and environmental protection are one of the great challenges. The combination of using liquid hydrogen (LH2) and polymer electrolyte membrane fuel cells (PEMFC) have recently attracted significant attention in the aviation industry due to its advantages such as the potential of zero greenhouse gases emission and high specific power compared to battery-based solutions. In this study, a system design to reuse the heat losses from fuel cell system for the vaporization and heating of LH2 is proposed in order to improve the overall energy efficiency of the fuel cell system. A control and optimization oriented dynamic model of a multi-modular PEMFC system and a LH2 tank system model in megawatt range are developed. By coupling of the PEMFC cooling system with the LH2 tank system, H2 preconditioning is simulated and analyzed. The goal of this work is to predict the supply temperature and pressure of hydrogen and investigate its effect on the fuel cell system performance and durability.

1. INTRODUCTION

The European Commission's Flightpath 2050 proposed a goal of reducing CO2 emissions by 75% and nitrogen oxide emissions by 90% per passenger kilometer [1]. In order to achieve this goal, fuel cell based electric powertrains are a promising technology [2]. Among various fuel cell types, the low-temperature polymer electrolyte membrane fuel cell (LT-PEMFC) stands out as a viable candidate for aviation applications due to its high volumetric and specific power density and technological maturity [3].

Hydrogen, the anode reactant of LT-PEMFC, can be stored either as liquid hydrogen (LH2) or as pressurized gas. Compared to gaseous hydrogen tanks, LH2 tanks offer higher hydrogen content while maintaining low weight and practical volume capacities [3] [4]. Thus, storing hydrogen as LH2 is attractive for aircrafts using LT-PEMFC as power system. LH2 is normally stored at a temperature of -253°C or lower [5]. Typical operation temperatures of LT-PEMFC are around 80°C and a proper humidification of reactants is required [6]. Operation of LT-PEMFC below −5°C can result in notable damage to both the membrane electrode assembly (MEA) and the backing layer components, according to ref. [7]. Hydrogen supplied at lower temperature may also cause water freezing in the fuel cell. When the temperature of the anode side is 5°C lower than that of the cathode side, water may accumulate at the anode side, which can increase the risk of local hydrogen starvation and fuel cell degradation [8]. The hydrogen pressure on the anode side of an LT/PEMFC is normally designed to be higher than the cathode pressure to prevent flooding at the anode and nitrogen crossover [9]. The experiment performed by Zhao *et al.* [10], shows the suitable range of pressure difference between the anode and cathode. Within 50 kPa pressure difference, a higher hydrogen pressure can improve the FC performance. Once the pressure difference exceeds 50 kPa, it shows that there is no significant improvement in the FC performance due to the increased hydrogen crossover. Excessive hydrogen crossover leads to an uncontrolled reaction between hydrogen and oxygen and consequently thermal degradation of the FC membrane [11]. Therefore, LH2 needs to be heated appropriately and vaporized before being supplied to LT-PEMFC. Maintaining the hydrogen at a suitable temperature and pressure is important for the fuel cell system (FCS) performance and durability.

Nonetheless, there are few studies that predict the hydrogen feed temperature and pressure with consideration of the interaction between the fuel cell system (FCS) and the LH2 tank. Hence, in this paper, we investigate a system design that is proposed based on the design of the 1st generation tank/PEMFC system integrated in the DLR facility BALIS [12] and reuses the heat losses from FCS to vaporize and heat LH2. To achieve this, a dynamic model of the multimodular PEMFC system and LH2 tank system is developed in Dymola, enabling simulation of the dynamic changes of hydrogen feed temperature and pressure.

2. MATHEMATICAL MODEL

2.1. System Model

Within the framework of the BALIS project, a megawatt

doi: 10.25967/610014

PEMFC system is designed by using multi-stack approaches and split into 2 FCS to explore different use cases and different interconnections of the components on the electrical side [12]. To achieve megawatt power and considering the current LT-PEMFC development status, one FCS consists currently of 6 FC modules (FCMs) with each ~100 kW of maximum power. An FCM converts roughly 40%-60% of the chemical energy into heat [13]. To improve the overall system efficiency, the heat loss of the FCS is reused to vaporize and heat LH2 via the thermal system. Figure 1 gives a schematic system overview for coupling 6 FCMs with the LH2 tank system. Two different cooling circuits are implemented for the thermal management of the FC systems. The first one cools the FC stacks (high temperature, HT cooling system) while the second one regulates the temperature of the cathode subsystem (low temperature, LT cooling system). Through the heat transfer fluid, the heat energy of the HT cooling system and LT cooling system is either reused to vaporize the LH2 or discharged into the atmosphere. In a first approach, the coupling of the cooling system of one FCS and the LH2 tank system is simulated in this paper.

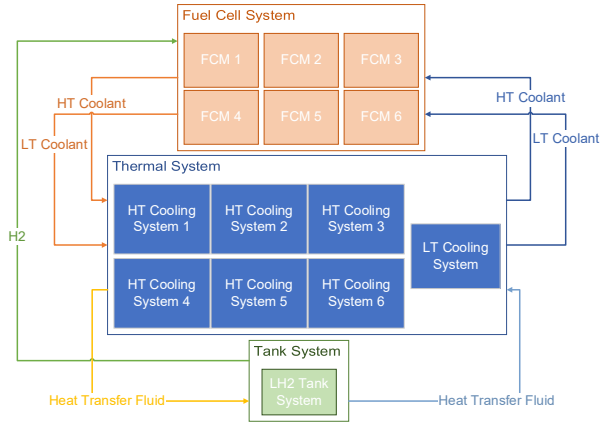

Figure 1 Schematic system overview

2.2. Fuel Cell Module Model

2.2.1. Model Assumption

The following assumptions are introduced to simplify the fuel cell module model:

- The anode, cathode and coolant paths of the PEMFC stack are treated as lumped volumes respectively neglecting the spatial variations.
- All gases are ideal gases and follow the ideal gas law.
- Diffusion of water and nitrogen crossover are not considered in the scope of this study.
- All of the unreacted hydrogen is recirculated by the recirculation pump.
- The temperature of the anode and cathode flows are assumed to be similar.
- All water produced at the cathode is assumed to be liquid.

2.2.2. Stack Model

The stack model used in this paper is based on experimental data of stack with given polarization curves. The cell voltage can be calculated with the polarization curve by giving the current density and the cathode pressure p_c. The stack voltage is determined as sum of the voltage of all cells.

The anode path is modeled as a single lumped volume with a pressure loss device between the inlet and the lumped volume. The mass balance equation for the anode lumped volume is as follow:

$$\frac{dm_{an}}{dt} = \dot{m}_{H_2,in} - \dot{m}_{H_2,out} - \dot{m}_{H_2,consumed} \quad (1)$$

$$\dot{m}_{H_2,consumed} = n_{cell} * M_{H_2} * \frac{I}{2 * F} \quad (2)$$

where m_{an} is the mass of hydrogen, $\dot{m}_{H_2,in}$ and $\dot{m}_{H_2,out}$ are the mass flow rates of hydrogen inlet and outlet flow respectively, $\dot{m}_{H_2,consumed}$ is the consumed hydrogen mass flow during reaction, n_{cell} is the number of cells, M_{H_2} is the molar mass of hydrogen, I is the stack load and F is Faraday's constant. The pressure drop dp_{H_2} in the anode channel is computed using a flow resistance component. This component uses quadratic approximation for the pressure loss and is expressed as follow:

$$dp_{H_2} = a * \dot{V}_{H_2}{}^2 + b * \dot{V}_{H_2} \quad (3)$$

where $\dot{V}_{H_2}$ is the volume flow rate of hydrogen, a and b are the linear and quadratic coefficients, which are determined by experimental data.

By applying a method similar to modeling the anode side, the mass balance equation and pressure drop dp_{ca} for the cathode side can be described by the following equations:

$$\frac{dm_{ca}}{dt} = \dot{m}_{ca,in} - \dot{m}_{ca,out} - \dot{m}_{O_2,consumed} + \dot{m}_{H_2O,prod} \quad (4)$$

$$\dot{m}_{O_2,consumed} = n_{cell} * M_{O_2} * \frac{I}{4 * F} \quad (5)$$

$$\dot{m}_{H_2O,prod} = n_{cell} * M_{H_2O} * \frac{I}{2 * F} \quad (6)$$

$$dp_{ca} = a * \dot{V}_{ca}{}^2 + b * \dot{V}_{ca} \quad (7)$$

where m_{ca} is the mass of air in the cathode, $\dot{m}_{ca,in}$ and $\dot{m}_{ca,out}$ are the mass flow rate of the air inlet and outlet flow respectively, $\dot{m}_{O_2,consumed}$ is the by reaction consumed oxygen mass flow, $\dot{m}_{H_2O,prod}$ is the produced water mass flow and $\dot{V}_{H_2}$ is the volume flow rate of air.

PEMFC converts the chemical energy from hydrogen and oxygen into electrical energy and heat. The heat energy is

part of the consumed chemical energy that is not converted into electrical energy and thus the heat production rate P_{heat} can be calculated as:

$$P_{heat} = P_{in} - P_{el} = (U_{thermoneutral} - U_{el}) * I * n_{cell} = \left(\frac{\Delta h}{nF} - U_{el}\right) * I * n_{cell} \quad (8)$$

where P_{in}, P_{el}, $U_{thermoneutral}$, U_{el} and Δh stand for the rate of energy input, electrical power, thermoneutral voltage, operating voltage and the specific enthalpy of reaction, respectively. It was assumed, that the heat dissipated to the ambient is zero. The stack thermal model contains the thermal mass of the anode, cathode, coolant volumes and the thermal mass of the stack solid material. All the heat that is produced by the reaction at the cathode is conducted to coolant, stack and exhaust gases. They are connected by heat conduction.

2.2.3. Anode Subsystem

The anode subsystem modeled in this paper has a dead-ended anode structure with periodic purging and consists of a pressure reducing valve, recirculation pump, mixed volume and purge valve. A schematic layout of the fuel cell system is shown in Figure 2. Gaseous hydrogen (GH2) is transported into the anode subsystem from the LH2 tank system at a pressure of about 6 bar. The hydrogen pressure is reduced by the pressure control valve so that the pressure difference between both sides of the membrane is maintained at a certain level to minimize the risk of gas crossover. Using the recirculation pump, the unreacted hydrogen is circulated. In the mixed volume, the recirculated hydrogen mixed with the fresh hydrogen. The purge valve is opened periodically to discharge the accumulated water and nitrogen, which are diffused from the cathode to the anode.

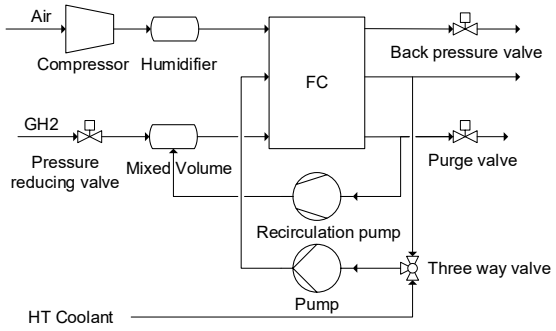

Figure 2 Schematic layout of the fuel cell system

Recirculation Pump

It was assumed that the temperature of the anode flow after passing through the recirculation pump remains the same. The mass flow rate of the recirculated hydrogen flow $\dot{m}_{H_2,recirculated}$ is described by:

$$\dot{m}_{H_2,recirculated} = \dot{m}_{H_2,consumed} * r_{recirculated} \quad (9)$$

where $r_{recirculated}$ is the ratio between the recirculated and consumed hydrogen amount. The pressure difference is a result of mass flow and connected components.

Pressure Control Valve

The pressure control valve is used to maintain the anode pressure at a specific level in the stack as the inlet pressure and the flow rate can fluctuate and change. This is accomplished by changing the valve opening degree. The anode flow rate and pressure vary due to changes in load demand or during the purge process. The valve position can be adjusted by comparing the anode pressure with setpoint. The mass flow rate through the valve is changed with the valve position. A proportional valve model with a PI-controller is used to simulate this process. The proportional relationship between pressure drop and the flowrate is described by:

$$\dot{m}_{H_2} = \alpha * k_h * dp \quad (10)$$

where k_h is the hydraulic conductance at full opening. α represents the opening degree of the valve.

Purge Valve

To remove the accumulated nitrogen in the anode loop, the anode purge valve is opened for a defined duration and frequency. The anode purge valve is closed in inactive state and can only be either fully opened or closed. The flow rate of purge flow $\dot{m}_{purge}$ is determined by the pressure difference dp between the valve inlet and valve outlet. For a compressible valve, the following equation is used:

$$\dot{m}_{purge} = \begin{cases} \alpha * Kv * Y * \sqrt{dp * \rho_1} & Valve\ open \\ 0 & Valve\ closed \end{cases} \quad (11)$$

where Y is the expansion factor, ρ_1 is the gas density at the valve inlet. The purge valve flow coefficient Kv is set to 1.6 m³/h.

Cathode Subsystem

Ambient air feed to the cathode subsystem is compressed by an air compressor first and then humidified in a humidifier. The feed demand of airflow $\dot{m}_{air,feed}$ is determined by:

$$\dot{m}_{air,feed} = \frac{I * n_{cell}}{4 * F * x_{O_2}} * \lambda_{cathode} * M_{air} \quad (12)$$

where $\lambda_{cathode}$ is the cathode stoichiometry, x_{O_2} is the oxygen content in air and M_{air} is the molar weight of air.

The temperature of air after the air compressor $T_{2,act}$ is calculated by the isentropic efficiency η_s and isentropic technical work w_{act}.

$$\begin{cases} w_s = c_{p,m} * T_1 * \left(\left(\frac{p_2}{p_1}\right)^{\frac{\kappa-1}{\kappa}} - 1\right) \\ w_{act} = c_{p,m} * (T_{2,act} - T_1) \\ \eta_s = \frac{w_s}{w_{act}} \end{cases} \quad (13)$$

Where T_1, p_1, p_2 stand for the inlet temperature, pressure and outlet pressure, $c_{p,m}$ is the specific heat capacity, κ is the ratio of specific heat for air. It was assumed that the airflow is well humidified and tempered by the LT coolant to reach the desired temperature.

The back pressure of the cathode is controlled by adjusting the opening degree of a simple valve model through a PI-controller and follows a defined dependency between the cathode pressure and the current density. The valve model describes a proportional relationship between pressure drop, the flow rate and the opening factor.

2.2.4. HT Cooling Subsystem

The heat produced by the electrochemical reaction in the stack is removed by the HT coolant. The HT cooling subsystem plays an important role to maintain the stack temperature in an optimum range. Higher temperature may cause membrane dehydration and lower temperature may induce flooding of the flow channel [14]. The flow rate of coolant in this study is controlled to ensure a constant temperature difference for the coolant between the stack inlet and outlet using PI-controller. The coolant inlet temperature is controlled by the bypass valve opening factor using PI-controller as well.

2.3. Hydrogen Tank System Model

Figure 3 illustrates a simplified P&ID of a pressurized LH2 storage system. The LH2 is stored in a cryogenic tank with a temperature of -245.5°C at 6 bar. During operation, hydrogen is withdrawn from the LH2 tank in its liquid state, since less vaporization is required in the tank to maintain the tank pressure at a desired level, compared to extracting hydrogen in gaseous state. The LH2 tank can be pressurized using an internal hydrogen vaporizer. An internal electric heater is used in the initial assumption. The LH2 flow is driven by the pressure differences between tank and anode and flows to an intermediate heating circuit first, where LH2 is vaporized and heated. The technology considered for the external vaporizer is a test unit and not an industry standard for this application. Therefore, leakages cannot be fully excluded. To prevent damage of the fuel cell system and the thermal facilities due to a possible leak, some precautions have been considered within the design. The intermediate heating circuit is designed at a pressure higher than the LH2 supply line to prevent gas leakage into the main thermal system. A downstream humidity sensor should detect any possible heat transfer fluid leakages into the hydrogen supply system. The intermediate heating circuit is heated continuously by the thermal system. During cold start, when the cooling system requires time to reach an optimum operating temperature, the heat transfer fluid to heat the intermediate circuit is warmed up by a 60-kW electric heater with on-off control and circulated without passing through the main thermal system. This ensures that the intermediate circuit receives immediate heat without waiting for the entire thermal system to reach its optimal operating temperature. After being sufficiently warmed up by the heat loss of FCS, the heat transfer fluid from the main thermal system is used to warm up the intermediate circuit.

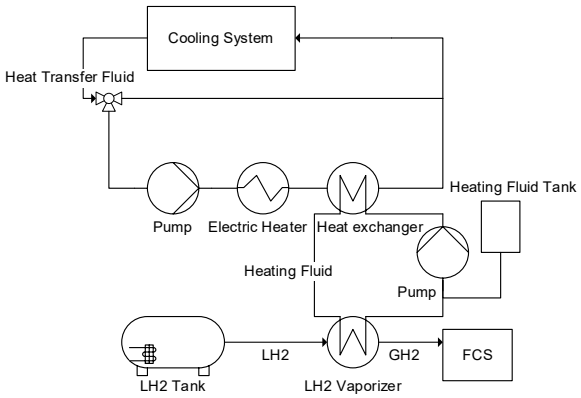

Figure 3 A simplified P&ID of a pressurized LH2 storage system

Tank Model

The tank model used in this study is developed by Riedel [15] and can only be used for two-phase media. In this tank model, one control volume (CV) for the gaseous, one for liquid phases and one for the interface between the phases are defined, in order to simulate the dynamic behavior of liquid and gaseous phases. The interface CV represents the saturated vapor at the tank pressure and enables to model the heat transfer through convection between gaseous hydrogen (GH2) and LH2. The mass and energy balance equations are solved for each CV respectively. More details on the tank model can be found in [15]. In Table 1, some assumed tank parameters are listed.

Mass of LH2 [kg]	207
Tank internal length [m]	2.25
Tank internal radius [m]	0.75
Tank pressure [bar]	6

Table 1 Geometry parameter of LH2 tank

LH2 Vaporizer

LH2 at a temperature of -245.5°C is vaporized by a shell and plate heat exchanger (SAPHX), which consists of chevron-type round plates. The heating fluid enters the SAPHX with an inlet temperature above 35°C. The inlet temperature difference between both fluids is therefore above 200 K. According to ref. [16], a vapor layer occurs across the surface of the wall. Therefore, it was assumed, that the heat transfer between the GH2 and the heating fluid is dominant. The heat flow from the environment is neglected as well. The P-NTU method, which describes the temperature effectiveness P as a function of NTU (number

of transfer unit) and R (ratio of the minimum and maximum heat capacity), is adopted to model the SAPHX and can be represented by the equation:

$$P = f(NTU, R, flow\ arrangement) \quad (14)$$

NTU is given by the ratio of the overall heat transfer coefficient and the heat transfer area. The heat transfer coefficient h is determined by the Nusselt number (Nu), which is given by

$$Nu = \frac{hD_h}{k} = 0.205 Pr^{\frac{1}{3}} (f * Re^2 sin2\beta)^{0.374} \quad (15)$$

where D_h is the hydraulic diameter, k is the thermal conductivity, Pr is the Prandtl number, Re is the Reynolds number and β is the chevron angle [17]. Since the frictional pressure drop is dominant [17], the pressure drop occurring at the inlet and outlet ports was not taken into account in this investigation. The pressure drop Δp is given by

$$\Delta p = \frac{G^2}{2g\rho_{in}} * \left(\frac{4fL\rho_{in}}{(\rho_{in} + \rho_{out})D_h} + 2\left(\frac{\rho_{in}}{\rho_{out}} - 1\right)\right), \quad (16)$$

where G is the fluid mass velocity, L is total duct length, ρ_{in} and ρ_{out} are the density at the inlet and outlet respectively. For a chevron angle within 0 to 80°, the friction factor f is given by:

$$f = \left(\frac{1}{\frac{\cos(\beta)}{(0.045\tan(\beta) + 0.09\sin(\beta) + \frac{f_0}{\cos(\beta)})^{0.5}} + \frac{1-\cos(\beta)}{\sqrt{3.81 f_1}}} \right)^2 \quad (17)$$

with

$$f_0 = \begin{cases} \frac{16}{Re} & Re < 2000 \\ (1.56 lnRe - 3)^{-2} & Re \geq 2000 \end{cases}$$

$$f_1 = \begin{cases} \frac{149.25}{Re} + 0.9625 & Re < 2000 \\ \frac{9.75}{Re^{0.289}} & Re \geq 2000 \end{cases}$$

2.4. Thermal System

Based on the design of the BALIS project, the heat loss of the FCS is either discharged to the atmosphere or transferred to the LH2 tank system via the main thermal system. As shown in Figure 4, the HT coolant and NT coolant are cooled by the heat transfer fluid in the heat exchangers. The temperature of HT coolant and NT coolant before entering the FCS is controlled by adjusting the flow rate of the heat transfer fluid using a PI-controller. Subsequently, a bypass flow of coolant is directed to heat the LH2 tank system. The heat transfer fluid flows together and dissipates all remaining rest heat losses through the dry cooler in the atmosphere. It was assumed, that the dry cooler is ideal and can cool the coolant to a desired temperature. Due to the significant computation time required by the current model, transport delay in the piping system is currently neglected.

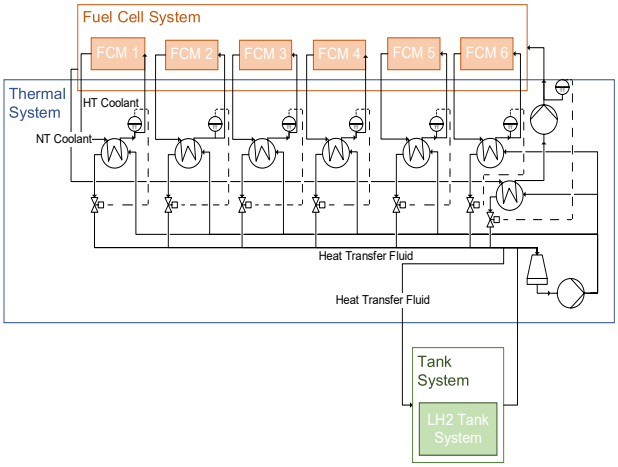

Figure 4 A simplified P&ID of the thermal system

Heat Exchanger Model

The heat exchanger model is taken from the Modelica Buildings Library [18] and uses the effectiveness ε and NTU relation for a plate heat exchanger. The transferred heat $\dot{Q}$ is determined by

$$\dot{Q} = \dot{Q}_{max} * \varepsilon \quad (18)$$

$$\varepsilon = f(NTU, R, flow\ arrangement) \quad (19)$$

where $\dot{Q}_{max}$ is the maximum heat that can be transferred.

For a given heat transfer flow data under nominal flow conditions, the convective heat transfer coefficient h is calculated by

$$\frac{h_1 A_1}{h_{1,nomial} A_{1,nominal}} = \left(\frac{\dot{m}_1}{\dot{m}_{1,nominal}}\right)^{n_1}, \quad (20)$$

which is derived from

$$h \propto k(\rho v x/\eta)^n Pr^{1/3} \quad (21)$$

$$\frac{h_1}{h_2} \propto \frac{k_1 \left(\frac{\dot{m}_1}{\eta_1}\right)^n Pr_1^{\frac{1}{3}}}{k_2 \left(\frac{\dot{m}_2}{\eta_2}\right)^n Pr_2^{\frac{1}{3}}} \quad (22)$$

where v is the flow velocity, x is the characteristic length and η is the dynamic viscosity.

Pump Model

The model of a centrifugal pump is described by the polynomial flow characteristic between the volume flow rate of the fluid, the rotation speed of the circulation pump and pressure ratio.

3. COMPONENT CONTROL

Anode Pressure Control

The anode pressure is set to follow the cathode pressure and maintain the pressure difference within a range of 0.2 bar [19] in order to prevent hydrogen crossover. The process is simulated by a proportion valve with a PI controller. The input of the PI controller is the measured anode pressure and the output is the valve opening degree. The proportional control gain minimizes the offset between the measured pressure and the setpoint while the integral control gain eliminates the offset. The Ziegler–Nichols method is applied to tune the PI-controller in order to yield a slightly oscillating control behavior of the anode pressure due to the influence of dead time.

LH2 Tank Pressure Build-up

To maintain the tank pressure during the operation, a heat flow is supplied to LH2 tank and adjusted by a PI controller. The integral control gain is adopted to eliminate the load change induced offset. The control target of the PI controller is to maintain the tank pressure at the specified tank pressure setpoint of 6 bar. The model does not considerate the inertia in translating these electrical signals into actuator actions. Additionally, the detailed heat transfer processes during LH2 boiling at the heating elements, which effects the process response time, are not considered.

4. PRELIMINARY RESULTS AND DISCUSSION

The model depicted in the front section is developed in Dymola. Full model validation has not been achieved yet. The validation of developed model is planned within later project stages on the BALIS test field. Currently, feasibility studies are made based on various literatures. The current model yields some preliminary results that contribute to gain some insight into the possible hydrogen temperature and pressure progression during a typical flight scenario.

The simulated load profile has been assumed on the basis of the flight data of Hy4 and is shown in Figure 5. The transition between the load states is ramped by a first order transfer function such that the ramp-up speed cannot exceed the maximum load increase, which is specified by the fuel cell manufacturer. We investigate the case, in which the purge rate is proportional to the stack current. At 50% current purge valve is opened for a duration of 0.2s every 6s. And there is a random time delay within 0s - 1s between master FCM und slave FCM (see Figure 6).

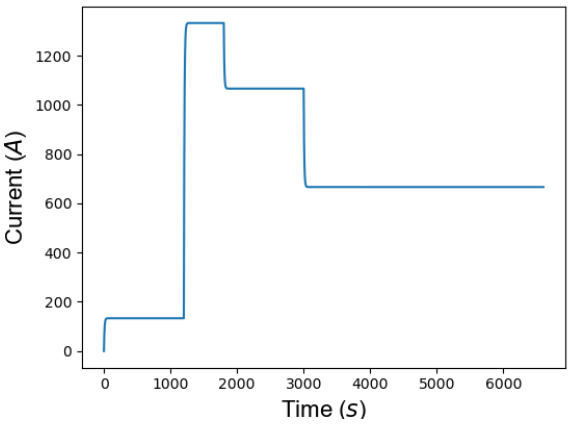

Figure 5 Load profile

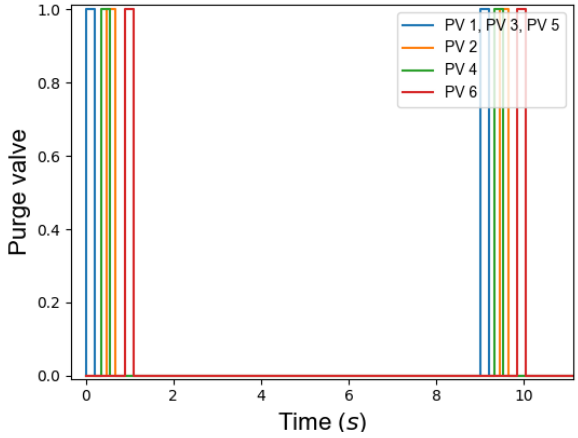

Figure 6 Purge cycle

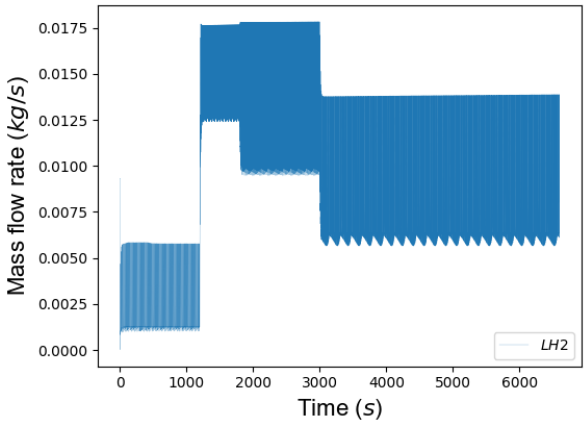

Figure 7 Mass flow rate of hydrogen during the operation

Figure 7 shows the simulated total feed mass flow of LH2 from the LH2 Tank into the 6 FCM during the operation. At the beginning of the operation, a high mass flow rate of LH2 is required in order to fill the whole anode volume of the FC stacks. After that, the mass flow of LH2 changes according to the flight phase respectively. Mass flow peeks can be seen for each purge period. The purge amount of hydrogen in the last three stages is significantly higher than first stage since the purge amount is calculated from the pressure

difference between standard atmospheric pressure 1.013bar and anode pressure, which is controlled to follow the cathode pressure.

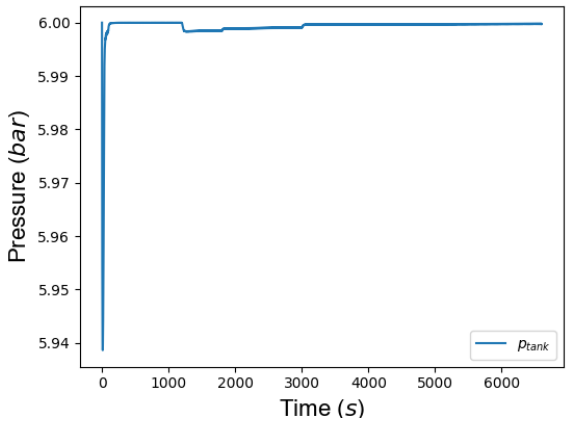

Figure 8 Pressure progression in LH2 tank

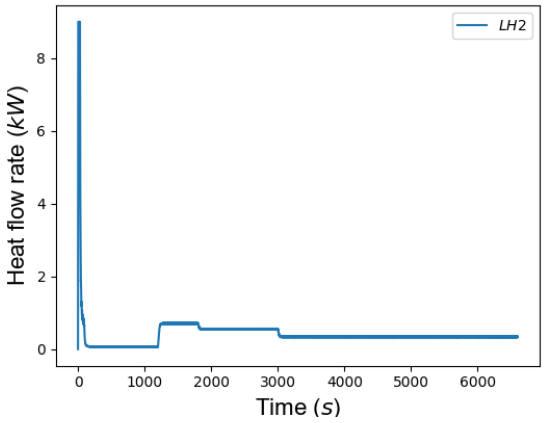

Figure 9 Heat flow rate for pressurization in LH2 tank

The pressure change of LH2 in the tank is presented in Figure 8. A highest fluctuation of about 60 mbar is shown at the beginning of the operation. In the reality, a lower fluctuation is expected, since the 12 modules will not be started simultaneously in normal circumstances. After that, the pressure remains relatively stable. A significant effect of LH2 feed demand change and purge process on the tank pressure are not observed in the simulation. The reason for that is, only half FC systems are simulated. Therefore, more heating power is available to maintain the desired pressure. As shown in Figure 9, only at the beginning of operation the maximum available heat flow rate of 9 kW is required for about 30s. After that, the required heat flow for pressurization is reduced within the 1 kW range. It is expected that the changes in the LH2 feed demand of entire system has a greater effect on the tank pressure. Furthermore, the actual process response time of a specified pressurization process is not considered due to lack of information about that. Further development of the model is required to account for more detailed pressurization process in LH2 tank. This can be achieved by using mathematical approximation model with experimental data or developing a more detailed physical model of LH2 tank.

Figure 10 compares the pressure of GH2 at the anode inlet with the anode pressure set point and the cathode inlet pressure. The anode pressure set point is 20 kPa higher than the cathode pressure according to ref. [19]. Although the simulated LH2 feed pressure is relatively stable, the anode pressure fluctuates significantly during each purge cycle. As shown in Figure 11, after the purge valve is opened, the anode pressure drops rapidly below the cathode pressure. Once the purge process is complete, the anode pressure rises slightly above the setpoint but still within the limit value given by [10], 50kPa.

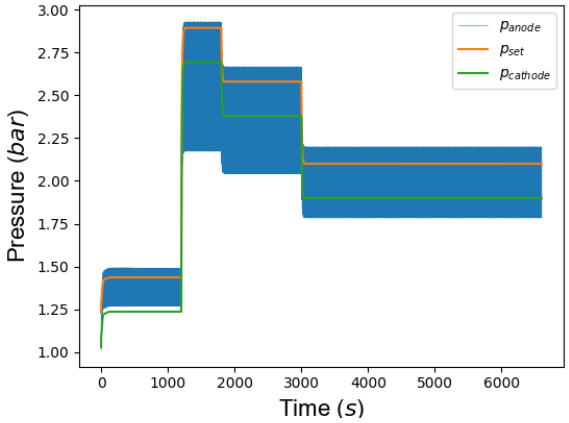

Figure 10 Pressure progression in anode, cathode and the reference value of anode pressure

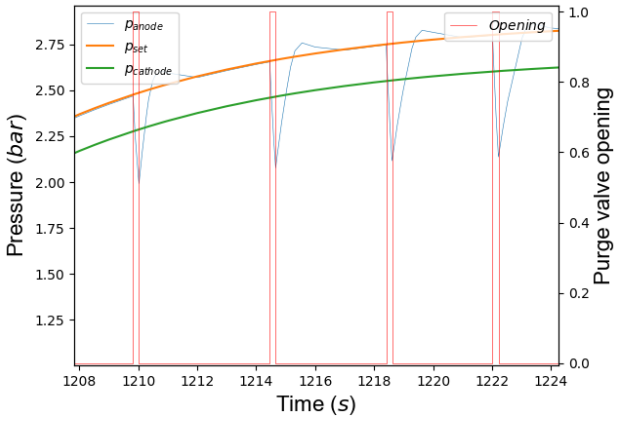

Figure 11 Pressure progression in anode, cathode and the reference value of anode pressure and the corresponding purge valve opening degree

The temperature progression of hydrogen at FCM inlet, anode inlet and anode outlet are illustrated in Figure 12. At cold start, it can be observed, that the temperature of H2 $T_{H2,FCS,in}$ at FCM inlet is below 0°C for about 2s due to the high hydrogen mass flow rate. If a drying procedure of the last operation is not executed properly, it may lead to the ice formation in the hydrogen water separator. After the heat transfer fluid is heated by the electric heater and its temperature fluctuates between 30°C and 38°C, the hydrogen feed temperature $T_{H2,FCS,in}$ is on the level between 6-13°C, which exceeds already the critical temperature. It may indicate, that at an ambient temperature of 20°C, the intermediate heating circuit should be preheated to a temperature higher than 30°C before FC

starts operating. More attention should still be paid to the low feed temperature of hydrogen and the consequently high temperature gradient between the air and hydrogen in further studies. The water transport from the cathode to the anode side could be enhanced by this temperature gradient [8]. Thus, the risk of the anode flooding should be investigated. After the heat transfer fluid is warmed up sufficiently, the heat loss of FCS is reused to vaporize the hydrogen. The hydrogen feed temperature increases gradually with the heat transfer fluid until 1200s when the load stage changes and higher hydrogen amount is required. Corresponding changes of hydrogen demand and the hydrogen feed temperature can be observed along with load stage variation. The temperature of hydrogen $T_{H2,anode,in}$ at the anode inlet, mixed with the recirculated hydrogen, is between 40°C – 60°C. Since the specific heat capacity of hydrogen is about 8 times higher than that of water, the effect of the neglected water on the results should be small. According to ref. [20], when hydrogen is humidified properly at the anode inlet temperature, the effect of anode temperature on the fuel cell performance is not significant at high current density. During the purge process, a lower temperature of hydrogen can be observed because of suddenly enhanced mass flow rate of hydrogen. However, a temperature below 20°C after the cold start is not observed. Hence, no significant impact on the fuel cell performance due to the LH2 feed demand change and purge process is observed and analyzed. However, again it must be pointed out that the current model does not describe all relevant processes adequately and further refinement is required.

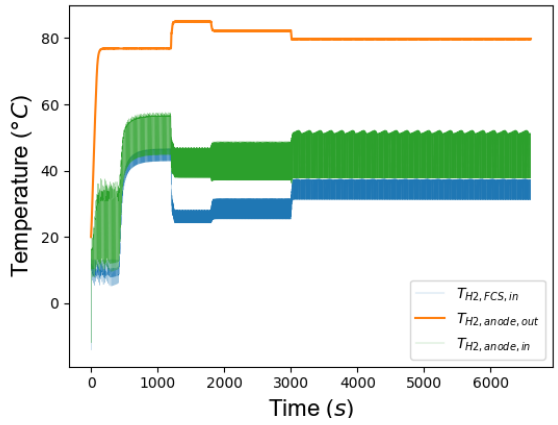

Figure 12 Temperature progression of hydrogen at FCM inlet, anode inlet and anode outlet

5. CONCLUSIONS AND OUTLOOK

In this paper, a dynamic model of a megawatt PEM fuel cell system with hydrogen supply from the LH2 tank is presented. The model simulates the supply temperature and pressure of hydrogen from the LH2 tank system. The effect of hydrogen temperature, pressure changes on the fuel cell performance is discussed by comparing with the literature.

The model developed in this paper requires further experimental validation. The ongoing construction of the BALIS test facility will provide an opportunity for comprehensive validation. Moreover, in order to simulate effects of hydrogen pressure, temperature and humidity on the fuel cell performance, further development of the FC stack model needs to be carried out. A more detailed and comprehensive voltage model that describes the fuel cell stack voltage as a function of the current demand, reactant pressure, temperature and humidity, should be implemented in the further work. Thereby, a water transport model should be also considered. To further investigate the interaction between FCS and LH2 tank, a model of the tank pressurization concept applied in BALIS should be developed. The thermal inertia of the system should also be investigated.

ACKNOWLEDGEMENTS

REFERENCES

[1] European Commission. Directorate General for Research and Innovation.; European Commission. Directorate General for Mobility and Transport. (2011). *Flightpath 2050 :Europe's Vision for Aviation : Maintaining Global Leadership and Serving Society's Needs.*, Publications Office, LU

[2] Sahoo, S.; Zhao, X.; Kyprianidis, K. (2020). A Review of Concepts, Benefits, and Challenges for Future Electrical Propulsion-Based Aircraft, *Aerospace*, Vol. 7, No. 4, 44. doi:10.3390/aerospace7040044

[3] Baroutaji, A.; Wilberforce, T.; Ramadan, M.; Olabi, A. G. (2019). Comprehensive investigation on hydrogen and fuel cell technology in the aviation and aerospace sectors, *Renewable and Sustainable Energy Reviews*, Vol. 106, 31–40. doi:10.1016/j.rser.2019.02.022

[4] Fuel Cells and Hydrogen 2 Joint Undertaking (EU body or agency) Now known as. (2020). *Hydrogen-Powered Aviation: A Fact Based Study of Hydrogen Technology, Economics, and Climate Impact by 2050*, Publications Office of the European Union, LU

[5] Rivard, E.; Trudeau, M.; Zaghib, K. (2019). Hydrogen Storage for Mobility: A Review, *Materials*, Vol. 12, No. 12, 1973. doi:10.3390/ma12121973

[6] Dicks, A.; Rand, D. A. J. (2018). *Fuel Cell Systems Explained* (Third edition.), Wiley, Hoboken, NJ, USA

[7] Yan, Q.; Toghiani, H.; Lee, Y.-W.; Liang, K.; Causey, H. (2006). Effect of sub-freezing temperatures on a PEM fuel cell performance, startup and fuel cell components, *Journal of Power Sources*, Vol. 160, No. 2, 1242–1250. doi:10.1016/j.jpowsour.2006.02.075

[8] Omrani, R.; Seif Mohammadi, S.; Mafinejad, Y.; Paul, B.; Islam, R.; Shabani, B. (2019). PEMFC purging at low operating temperatures: An experimental approach, *International Journal of Energy Research*, er.4783. doi:10.1002/er.4783

[9] Chen, W.; Liu, Y.; Chen, B. (2022). Numerical Simulation on Pressure Dynamic Response Characteristics of Hydrogen Systems for Fuel Cell Vehicles, *Energies*, Vol. 15, No. 7, 2413. doi:10.3390/en15072413

[10] Zhao, C.; Xing, S.; Liu, W.; Wang, H. (2020). Comprehensive Anode Parameter Study for an Open-Cathode PEMFC, *Energy & Fuels*, Vol. 34, No. 6, 7582–7590. doi:10.1021/acs.energyfuels.0c01083

[11] Tang, Q.; Li, B.; Yang, D.; Ming, P.; Zhang, C.; Wang, Y. (2021). Review of hydrogen crossover through the polymer electrolyte membrane, *International Journal of Hydrogen Energy*, Vol. 46, No. 42, 22040–22061. doi:10.1016/j.ijhydene.2021.04.050

[12] Fritz, J.; Bänsch, C.; Weiss, J.; Hacker, G.; Diarra, D.; Bever, C.; Thiele, I. (2022). Systems Engineering Methodology on a Multi-Integration Test Environment for Fuel Cell Flight Propulsion Systems, 7 pages. doi:10.25967/570366

[13] Kazula, S.; Graaf, S. de; Enghardt, L. (2023). Review of fuel cell technologies and evaluation of their potential and challenges for electrified propulsion systems in commercial aviation, *Journal of the Global Power and Propulsion Society*, Vol. 7, 43–57. doi:10.33737/jgpps/158036

[14] Li, Q.; Liu, Z.; Sun, Y.; Yang, S.; Deng, C. (2021). A Review on Temperature Control of Proton Exchange Membrane Fuel Cells, *Processes*, Vol. 9, No. 2, 235. doi:10.3390/pr9020235

[15] Riedel, S. (n.d.). *Simulation-Based Design of a Liquid Hydrogen Storage System Architecture for Aviation Applications Considering Dynamics*

[16] Shenton, M.; Leachman, J. (2022). A Review on Liquid Hydrogen Pool-Boiling Correlations, *IOP Conference Series: Materials Science and Engineering*, Vol. 1240, No. 1, 012152. doi:10.1088/1757-899X/1240/1/012152

[17] Shah, R. K.; Sekulić, D. P. (2003). *Fundamentals of Heat Exchanger Design*, John Wiley & Sons, Hoboken, NJ

[18] Wetter, M.; Zuo, W.; Nouidui, T. S.; Pang, X. (2014). Modelica Buildings library, *Journal of Building Performance Simulation*, Vol. 7, No. 4, 253–270. doi:10.1080/19401493.2013.765506

[19] PowerCellution: P System 100 Extended Product Sheet. (n.d.)

[20] Wang, L. (2003). A parametric study of PEM fuel cell performances, *International Journal of Hydrogen Energy*, Vol. 28, No. 11, 1263–1272. doi:10.1016/S0360-3199(02)00284-7